

Distribution-free Phase II Mann-Whitney Control Charts with Runs-rules

J.C. Malela-Majika^a

S. Chakraborti^{b,a}

M.A. Graham^{a,c}

jcmalela2005@yahoo.fr

schakrab@cba.ua.edu

marien.graham@up.ac.za

Abstract

The addition of runs-rules has been recommended to improve the performance of classical, normal theory Shewhart-type control charts, for detecting small to moderate size shifts. In this paper, we consider adding both standard and improved runs-rules to enhance the performance of the distribution-free Phase II Shewhart-type chart based on the well-known Mann-Whitney statistic proposed by Chakraborti and Van de Wiel [1]. Standard runs-rules are typically of the form w -of- $(w+v)$ with $w > 1$ and $v \geq 0$ and the improved runs-rules scheme is a combination of the classical 1 -of- 1 runs-rule and the w -of- $(w+v)$ runs-rules. The improved scheme improves the performance of the charts in detecting larger shifts while maintaining its performance in detecting small to moderate shifts. The in-control and out-of-control performance of the proposed runs-rules enhanced distribution-free charts are examined through extensive simulations. It is seen that the proposed charts have attractive performance compared to some competing charts, and are better in many cases. An illustrative example is provided, along with a summary and conclusions.

Keywords: Case U, Improved Runs-rules, Mann-Whitney test, Shewhart-type chart.

1. Introduction

During the last decade, distribution-free (nonparametric) control charts have become increasingly popular. These charts are useful when the underlying distribution is not known and have been shown to perform well compared to their normal theory counterparts. Nonparametric control charts are often designed by adapting corresponding nonparametric hypothesis tests. It may be noted that remarkably, even when the underlying distribution is normal, the efficiency of some nonparametric tests, relative to their normal theory counterparts, can be as high as 0.955 (see e.g. Gibbons and Chakraborti [2] page 218). For some other heavy-tailed and skewed distributions, the efficiency can be 1.0 or even higher. It may be argued that nonparametric methods will be ‘less efficient’ than their parametric counterparts when one has a complete

^a Department of Statistics, University of Pretoria, South Africa

^b Department of Information Systems, Statistics and Management Science, University of Alabama, Tuscaloosa, AL 35487, U.S.A.

^c Corresponding author: Dr MA Graham, +27 (0) 12 420 4621 (phone), +27 (0) 12 420 5175 (fax), marien.graham@up.ac.za (email)

knowledge of the process distribution for which that parametric method was specifically designed. However, the reality is that such information is seldom, if ever, available in practice.

Over the last decade or so, many nonparametric control charts have been proposed in Statistical Process Control (SPC). Their advantages are listed in Chakraborti et al. [12] and are as follows: (i) easy to implement, i.e. simplicity; (ii) no need to assume a particular parametric distribution for the underlying process; (iii) the IC run-length distribution is the same for all continuous distributions; (iv) more robust and outlier resistant; (v) more efficient in detecting changes when the true distribution is markedly non-normal, particularly with heavier tails, and (vi) no need to estimate the variance to set up charts for the location parameter. For a thorough account on nonparametric control chart literature, including some recent developments, the reader is referred to Chakraborti et al. [12], Chakraborti and Graham [13] and Chakraborti et al. [14].

Among the many nonparametric control charts, the Mann-Whitney (hereafter MW) control chart, based on the well-known Mann-Whitney test (see Gibbons and Chakraborti [2]) is one of the most powerful due to its in-control (IC) robustness and good out-of-control (OOC) performance. Park and Reynolds [3] considered Shewhart-type charts for monitoring the location parameter of a continuous process in where the process parameters are unknown, and the MW chart based on the MW-Wilcoxon statistic is one of their special cases. However, they only considered properties of this chart when the reference sample size approaches infinity. Chakraborti and van de Wiel [1] considered the Shewhart-type MW chart for a finite reference sample size and studied its properties in more details. They showed that, in many cases, the MW chart performs better than the competing charts no matter the nature of the underlying process distribution. Among other uses of the MW statistic, a change-point formulation was investigated by Zhou et al. [4]. Li et al. [5] proposed a nonparametric cumulative sum (CUSUM) chart and a nonparametric exponentially weighted moving average (EWMA) control chart based on the Wilcoxon rank-sum (WRS) statistic W , respectively, with the W statistic being equivalent to the MW statistic.

In many settings, however, the Shewhart-type charts remain the most popular due to their operational simplicity and global performance. In order to improve their performance in detecting small to moderate shifts, the addition of runs-type signaling rules (in short, runs-rules) has been recommended for the normal theory Shewhart-type charts. The use of runs-rules with

the Shewhart \bar{X} chart, to increase its sensitivity in detecting small shifts, has been studied by Champ and Woodall [6]. These runs-rules are typically of the form w -of- $(w+v)$ with $w > 1$ and $v \geq 0$. More recently, Klein [7] proposed runs-rules with $w = 2$ and $v = 0$ and 1 , respectively, leading to the well-known 2 -of- 2 and 2 -of- 3 runs-rules. Khoo and Ariffin [8] proposed an improved runs-rules scheme which is a combination of the classical 1 -of- 1 runs-rule and the w -of- $(w+v)$ runs-rules. Koutras et al. [9] reviewed the well-known Shewhart-type charts supplemented with additional rules based on the theory of runs and scans. A class of Phase II nonparametric charts based on precedence statistics with runs-rules was proposed by Chakraborti et al. [10]. Zhang and Castagliola [11] investigated the runs-rules based Shewhart \bar{X} charts when process parameters are unknown. However, to date, runs-rules have not been applied to the Shewhart-type MW chart studied by Chakraborti and Van de Wiel [1]. In this paper we fill this gap by proposing and studying a class of nonparametric control charts with runs-rules where the charting statistic is based on the MW test statistic.

The performance of control charts depends on many factors such as: the type of chart, the nature of the underlying process distribution, the charting statistic, etc. In order to implement a control chart we need at least one sample observed on a particular quality characteristic from which the charting statistic is calculated. Nonparametric charting statistics are mostly based on two-sample tests. This is for Case U where the process parameter(s) is/are unknown. The MW chart is based on the MW test, which is one of the most popular nonparametric tests for light tailed distributions (see Gibbons and Chakraborti [2] page 261). Thus, the MW control chart is expected to be more powerful than many other control charts in this case. We describe the details in the next section.

2. Mann-Whitney control chart

2.1 MW charting statistics

These charts are to monitor the location parameter in the unknown parameter case (so-called Case U) where a reference sample is assumed to be available after a Phase I analysis. Assume that a reference sample of size m , say, X_1, X_2, \dots, X_m , is available from an IC process with an unknown continuous cdf $F(x)$. Let $Y_1^h, Y_2^h, \dots, Y_n^h, h = 1, 2, \dots$, denote the h^{th} test sample of size $n_h, n_h = n \forall h$, since we are assuming that the Phase II samples are all of the same size. Let $G^h(y)$ denote the cdf of the distribution of the h^{th} Phase II sample and let $G^h(y) = G(y) \forall h$, since the Phase II samples are all assumed to be identically distributed. The process is IC in

Phase II when $G = F$. Typically, the location model is assumed, that is $G(t) = F(t - \delta)$, for all t , where δ is the location difference (or shift in the location parameter). In that case the process is IC when $\delta = 0$.

The MW charting statistic M_{XY} represents the total number of (X_i, Y_j) pairs where the Y -observation (Phase II sample) is strictly greater than the X -observation (Phase I sample). This is defined by

$$M_{XY} = \sum_{i=1}^m \sum_{j=1}^n I(Y_j > X_i) \quad (1)$$

where $I(Y_j > X_i)$ is an indicator function defined as follows

$$I(Y_j > X_i) = \begin{cases} 1 & \text{if } Y_j > X_i \\ 0 & \text{if } Y_j \leq X_i \end{cases} \quad (2)$$

Note that there are mn (X_i, Y_j) pairs for each Phase II sample, therefore, $0 \leq M_{XY} \leq mn$. For the two most extreme orderings every x precedes every y (so that $M_{XY} = 0$) and every y precedes every x (so that $M_{XY} = mn$). The proposed charting statistics are given by, $M_{XY}^1, M_{XY}^2, \dots$.

2.2 Control limits

When implementing the MW control chart, we plot the charting statistics M_{XY}^h ($h = 1, 2, \dots$) for each test sample h . The classical *I-of-I* MW chart studied by Chakraborti and Van de Wiel [1] signals if the charting statistic falls on or above the upper control limit (*UCL*) or if the charting statistic falls on or below the lower control limit (*LCL*). Since the IC distribution of the charting statistic M_{XY} is symmetric about $\frac{mn}{2}$, the control limits are taken to be symmetrical. By means of the symmetry property (see Gibbons and Chakraborti [2] page 264), we have $P(M_{XY} = a) = P(M_{XY} = mn - a)$ for $0 \leq a \leq mn$ when the process is IC. Thus we set $LCL = mn - UCL$. If the charting statistic falls between the control limits, that is, $LCL < M_{XY} < UCL$, the process is declared to be IC, otherwise the process is declared OOC.

2.3 Run-length (N) and Average Run-Length (ARL)

The reader is referred to Chakraborti and Van de Wiel [1] for more details. Here we only give some key concepts. Let $p_G(\underline{x}) = P_G(M_{\underline{x}Y} \leq mn - UCL) + P_G(M_{\underline{x}Y} \geq UCL)$ denotes the probability of a signal with any test (Phase II) sample, given the reference sample $(X_1, X_2, \dots, X_m) = (x_1, x_2, \dots, x_m)$ denoted $\underline{X} = \underline{x}$. Therefore, the conditional run-length distribution is given by

$$P(N = k | \underline{X} = \underline{x}) = \left(1 - p_G(\underline{x})\right)^{k-1} \left(p_G(\underline{x})\right) \text{ for } k = 1, 2, \dots \quad (3)$$

Let N denote the run-length random variable for the chart given the reference sample $\underline{X} = \underline{x}$. N is geometrically distributed with parameter $p_G(\underline{x})$. Consequently, the conditional ARL is given by

$$CARL = E_G(N|\underline{X} = \underline{x}) = \frac{1}{p_G(\underline{x})}. \quad (4)$$

On the other hand, using Expression (4) and integrating over the distributions of the reference samples, the unconditional ARL is found to be

$$UARL = E_F[E_G(N|\underline{X} = \underline{x})] = E_F\left(\frac{1}{p_G(\underline{x})}\right) = \int_{-\infty}^{\infty} \dots \int_{-\infty}^{\infty} \frac{1}{p_G(\underline{x})} dF(x_2) \dots dF(x_m). \quad (5)$$

Note that Expression (5) is an m -dimensional integral, moreover we do not have an exact formula for the probability of a signal. Accordingly it is difficult and time-consuming to estimate the unconditional ARL using this formula. To overcome these problems, Chakraborti and Van de Wiel [1] proposed using Monte Carlo simulations or a Markov chain approach. Using a Markov chain approach, one has to do matrix inversion which can be very time consuming, particularly for large matrices. For this reason, in this paper we used Monte Carlo simulation with 10000 simulations.

2.3.1 In-Control ARL

In Phase II, the process is IC when $F = G$. Therefore, the unconditional IC ARL is found by substituting $G = F$ into Expression (5).

$$UARL_0 = \int_{-\infty}^{\infty} \dots \int_{-\infty}^{\infty} \frac{1}{p_F(\underline{x})} dF(x_2) \dots dF(x_m). \quad (6)$$

Expression (6) can be re-written, using the probability integral transformation, as:

$$UARL_0 = \int_{-\infty}^{\infty} \dots \int_{-\infty}^{\infty} \frac{1}{p_U(\underline{u})} du_1 \dots du_m. \quad (7)$$

For more details the reader is referred to Gibbons and Chakraborti [2] page 39. The subscript U refers to the $U(0,1)$ distribution and $p_U(\underline{u})$ is the conditional probability of a signal at any test sample, given the reference sample, when the process is IC.

2.3.2 Out-of-Control ARL

In the OOC case, $G \neq F$, the unconditional OOC ARL is given by

$$UARL_{\delta} = \int_{-\infty}^{\infty} \dots \int_{-\infty}^{\infty} \frac{1}{p_G(\underline{x})} dF(x_2) \dots dF(x_m), \quad (8)$$

where $\delta(\neq 0)$ represents the shift between F and G , in their location parameters. Thus, in order to implement the MW chart we have to calculate the $UARL_0$ and in order to evaluate the performance of the MW chart we have to evaluate the $UARL_{\delta}$. Using a similar argument as

earlier, it will not be easy to calculate these using Expressions (7) and (8) and, accordingly, we use Monte Carlo simulations. This will be explained in more detail later on.

3. Runs-Rules and Enhancements of the MW Chart

The classical *1-of-1* rule, i.e. when only one charting statistic is considered, as considered in Chakraborti and Van de Wiel [1], will be denoted by RR_{1-of-1} from this point forward. When considering the *2-of-2* runs-rule, which gives a signal when two consecutive charting statistics plot OOC, there is a distinction in the literature between the *2-of-2* runs-rules proposed by Klein [7], denoted KL (see (a) below), and the *2-of-2* runs-rules proposed by Derman and Ross [15], denoted DR (see (b) below). The formal definitions are given as follows.

- (a) Two consecutive points both fall on or above the UCL or both fall on or below the LCL (KL scheme).
- (b) Two consecutive points (i) both fall on or above the UCL or, (ii) both fall on or below the LCL or, (iii) one falls on or above the UCL and the next one falls on or below the LCL or, (iv) one falls on or below the LCL and the next falls on or above the UCL (DR scheme).

Chakraborti et al. [10] showed that the KL scheme outperforms the DR scheme and, accordingly, only the KL scheme is considered in this paper. The *2-of-2* KL runs-rule will be denoted by RR_{2-of-2} from this point forward. The improved runs-rules of Khoo and Ariffin [8], which is a combination of the classical *1-of-1* runs-rule and the *2-of-2* runs-rule, will be denoted by IRR_{2-of-2} . These rules are described below.

3.1 The RR_{1-of-1} , the RR_{2-of-2} and the IRR_{2-of-2} MW control chart

Rule 1: RR_{1-of-1}

The RR_{1-of-1} scheme signals when the charting statistic M_{XY} plots on or above the UCL_1 or plots on or below the LCL_1 . The subscript refers to the rule number. The use of subscripts is necessary in order to emphasize the fact that the values of the control limits for the three rules are not equal.

Rule 2: RR_{2-of-2}

The RR_{2-of-2} scheme signals when two consecutive charting statistics, say M_{XY}^h and M_{XY}^{h+1} for $h = 1, 2, \dots$, both plot on or above the UCL_2 or both plot on or below the LCL_2 .

Rule 3: IRR_{2-of-2}

For the IRR_{2-of-2} scheme some warning limits are introduced, namely, the UWL_3 and the LWL_3 , where $LCL_3 < LWL_3 < UWL_3 < UCL_3$. The improved runs-rules signal when one charting

statistic M_{XY} plots on or above UCL_3 or plots on or below LCL_3 or when two consecutive charting statistics, say M_{XY}^h and M_{XY}^{h+1} , for $h = 1, 2, \dots$, plot between $[UWL_3, UCL_3)$ or between $(LCL_3, LWL_3]$.

4. Implementation of the MW control chart with runs-rules

4.1 Monte Carlo simulation

The steps for determining the chart constants (control limits) and for obtaining the characteristics of the run-length distribution are given for the RR_{2-of-2} scheme; it can easily be amended to include warning limits for the IRR_{2-of-2} scheme.

Step 1: Specify two distributions for generating a Phase I and Phase II sample, respectively.

For the IC case, the two distributions are identical (we say that the shift equals zero ($\delta = 0$)). For the OOC case, the distribution for the Phase II sample is taken to be the same form as that for the Phase I sample, but with a shift in the location parameter in units of the population standard deviation. For example, the Phase I sample may be drawn from a normal distribution with mean 0 and standard deviation 1, whereas, in the OOC case, the Phase II sample may be drawn from a normal distribution with mean $\neq 0$ and standard deviation 1 (we say that the shift in the location (mean), δ , is not equal to zero ($\delta \neq 0$)).

Step 2: Specify the Phase I reference sample size (m), the Phase II test sample size (n), the number of simulations (r) and the parameter(s) of the distribution. For example, suppose we have a reference sample of size 100 with mean 0 and standard deviation 1, a test sample of size 5 with mean δ and standard deviation 1 and 10000 simulations are used, then $\delta = 0$ (0.25) 3, $m = 100$, $n = 5$ and $r = 10000$. In the IC case $\delta = 0$ while in the OOC case $\delta \neq 0$.

Step 3: The UCL_2 can take on any integer value in the range $\left[\frac{mn}{2} + 1, mn - 1\right]$. Thus, we vary UCL_2 from the smallest integer in the specified range to the largest integer in increments of 1. In our example, with $m = 100$ and $n = 5$, the UCL_2 can take on any integer value in the range [251,499].

Step 4: Randomly generate a Phase I sample from a distribution, such as the $N(0,1)$ distribution.

Step 5: For any given value of the UCL_2 , specified in Step 3, calculate its corresponding $LCL_2 = mn - UCL_2$. For example, say $UCL_2 = 300$, then we have $LCL_2 = (100)(5) - 300 = 200$ for $m = 100$ and $n = 5$.

Step 6: Randomly generate a Phase II test sample from the same distribution. Calculate the first MW charting statistic (point) using Expression (1) and compare it to the control limits obtained in Step 5. If this first point plots between the control limits we have to generate the next test sample, calculate the next point and compare it to the control limits obtained in Step 5. Continue this process until a point plots beyond the control limits. Once we get such a point, we again generate a new test sample and calculate the new point. The chart signals if both charting statistics (the previous and the new one) plot on or above (below) the UCL_2 (LCL_2). If this does not happen, then continue with the process until the chart signals for the first time and record the number of subgroups needed to get to that stage. In our example, after generating the first Phase II test sample, the first charting statistic (M_{XY}^1) is calculated. This is compared to the control limits $LCL_2 = 200$ and $UCL_2 = 300$. If $M_{XY}^1 \leq 200$ or $M_{XY}^1 \geq 300$ we generate a second Phase II test sample and calculate a second charting statistic (M_{XY}^2). The latter is compared to the control limits and, if it is also less than or equal to 200 ($M_{XY}^2 \leq 200$) or if it is also greater than or equal to 300 ($M_{XY}^2 \geq 300$) the chart signals. The run-length will equal two because we needed two Phase II test samples in order to get a signal. On the other hand, assume that the second charting statistic plotted between the control limits. Then, we need to generate new Phase II test samples until we get a charting statistic less than (greater than) or equal to 200 (300). Once we obtain such a charting statistic, generate the next test sample and calculate the corresponding charting statistic. Compare the new charting statistic to 200 and 300. Then, the chart signals if the new charting statistic plots below (above) the 200 (300) as well. Record the number of subgroups needed until we get a signal for the first time. This number represents one value of the run-length distribution.

Step 7: Repeat Step 6 a total of r times.

Step 8: Once the run-length values are obtained, calculate

$$ARL = \frac{1}{r} \sum_{i=1}^r RL_i. \quad (9)$$

- Step 9:** Record the LCL_2 and the UCL_2 values next to the ARL value (for $\delta = 0$ this will be the IC ARL).
- Step 10:** Repeat Steps 5 to 9 until all the values of UCL_2 allocated in Step 3 are considered.
- Step 11:** Select the control limits for which the IC ARL is closest to the nominal value of 500.
- Step 12:** Repeat Steps 4 to 8 using the control limits found in Step 11 by varying the shift $\delta = 0(0.25)3$ where $\delta = 0$ provides IC values and $\delta \neq 0$ provides OOC values. Record the IC and OOC ARL values.

Some illustrative examples are given below.

Example 1

For Rule 1, the RR_{1-of-1} scheme, with $(m, n) = (20, 5)$, the attained $ARL_0 = 426.77$ for $UCL_1 = 87$ and $LCL_1 = 20(5) - 87 = 13$. For a different combination of m and n , say $(m, n) = (100, 5)$, the attained $ARL_0 = 499.36$ for $UCL_1 = 436$ so that $LCL_1 = (100)(5) - 436 = 64$.

Example 2

For Rule 2, the RR_{2-of-2} scheme, with $(m, n) = (20, 5)$, the attained $ARL_0 = 431.07$ for $UCL_2 = 75$ and $LCL_2 = 20(5) - 75 = 25$. For a different combination of m and n , say $(m, n) = (100, 5)$, the attained $ARL_0 = 508.42$ for $UCL_2 = 373$ so that $LCL_2 = (100)(5) - 373 = 127$.

From Examples 1 and 2 it can be seen that, as the size of the reference sample (m) increases, the attained ARL_0 values tend to get closer to the nominal desired value of 500, i.e. the charts perform better, as expected nominally, for larger values of m .

Example 3

For Rule 3, the IRR_{2-of-2} scheme, with $(m, n) = (500, 5)$, the attained $ARL_0 = 496.32$ for $LCL_3 = 650$, $LWL_3 = 326$, $UWL_3 = 1850$ and $UCL_3 = 2174$.

Table 1 presents the chart constants (or control limits) and the corresponding attained ARL_0 values for different values of m and n , for the RR_{1-of-1} , the RR_{2-of-2} and the IRR_{2-of-2} schemes, respectively.

Table 1. Control limits and attained ARL_0 values for the three rules, the RR_{1-of-1} , the RR_{2-of-2} and the IRR_{2-of-2} schemes, for the Shewhart MW chart for different values of m and n .

Schemes		RR_{1-of-1}			RR_{2-of-2}			IRR_{2-of-2}				
m	n	LCL_1	UCL_1	Attained ARL_0	LCL_2	UCL_2	Attained ARL_0	LCL_3	LWL_3	UWL_3	UCL_3	Attained ARL_0
20	5	13	87	426.77	25	75	431.07	13	25	75	87	454.06
	10	44	156	525.16	63	137	472.80	44	63	137	156	492.38
	25	159	341	463.00	189	311	494.36	159	189	311	341	476.43
25	5	16	109	478.43	31	94	487.70	16	31	94	109	486.14
	10	55	195	487.63	79	171	511.22	55	79	171	195	506.72
	25	196	429	472.18	237	388	505.74	196	237	388	429	507.18
50	5	32	218	472.55	63	187	481.01	32	63	187	218	497.03
	10	110	390	491.82	159	341	507.40	110	159	341	390	508.95
	25	391	859	497.17	476	774	524.82	391	476	774	859	513.61
75	5	47	328	508.73	95	280	512.29	47	95	280	328	513.17
	10	167	583	506.96	241	509	509.73	167	241	509	583	508.30
	25	590	1285	528.43	716	1159	523.58	590	716	1159	1285	510.07
100	5	64	436	499.36	127	373	508.42	64	127	373	436	498.86
	10	224	776	492.95	323	677	484.23	224	323	677	776	493.56
	25	793	1707	501.51	960	1540	504.14	793	960	1540	1707	509.87
125	5	80	545	492.68	160	465	499.92	80	160	465	545	496.09
	10	279	971	503.86	405	845	483.67	279	405	845	971	504.56
	25	992	2133	505.06	1204	1921	511.54	992	1204	1921	2133	510.64
150	5	97	653	489.83	192	558	501.33	97	192	558	653	503.40
	10	332	1168	502.40	486	1014	507.28	332	486	1014	1168	516.01
	25	1190	2560	510.12	1443	2307	502.33	1190	1443	2307	2560	513.26
200	5	130	870	512.44	257	743	504.73	130	257	743	870	503.58
	10	446	1554	498.33	650	1350	500.61	446	650	1350	1554	505.26
	25	1595	3405	501.76	1934	3066	505.70	1595	1934	3066	3405	518.14
250	5	161	1089	515.13	323	927	501.74	161	323	927	1089	509.84
	10	559	1941	521.56	819	1681	500.02	559	819	1681	1941	506.71
	25	1970	4550	513.52	2423	3827	484.23	1970	2423	3827	4550	488.16
500	5	326	2174	498.20	650	1850	493.10	326	650	1850	2174	500.21
	10	1125	3875	501.50	1648	3352	491.83	1125	1648	3352	3875	503.04
	25	4016	8484	492.46	4855	7645	519.89	4016	4855	7645	8484	507.05

In Section 5 a performance comparison among the proposed runs-rules enhanced MW charts is done. We also include, in the comparison study, the distribution-free precedence charts proposed by Chakraborti et al. [10]. Note that although these authors considered the RR_{2-of-2} scheme, they did not consider the improved runs-rules and, accordingly, for the performance comparison we used the improved precedence chart proposed by Malela-Majika et al. [16].

Since obtaining the control limits is often time-consuming, we propose an approximation using regression, fitting a straight line between the Phase I sample size (the explanatory variable) and the upper control limit (the dependent variable). For example, with the data at our disposal for Rule 2, the RR_{2-of-2} scheme, for the Shewhart MW chart (see Table 1, first and seventh columns for $n = 5$), the least squares regression line is given by $\widehat{UCL}_2 = 2.6682868 + 3.7000365m$ and hence $\widehat{LCL}_2 = mn - \widehat{UCL}_2$ where \widehat{LCL}_2 and \widehat{UCL}_2 denote the estimated lower and upper control limits, respectively. Similarly, for Rule 1, the RR_{1-of-1} scheme, for the Shewhart MW chart (see Table 1, first and fourth columns for $n = 5$) the fitted line is given by $\widehat{UCL}_1 = 0.908363 + 4.349375m$ and $\widehat{LCL}_1 = mn - \widehat{UCL}_1$. For the IRR_{2-of-2} scheme, for the Shewhart MW chart (see Table 1), the estimated least squares regression lines for the upper warning and upper control limits are respectively given by $\widehat{UWL}_3 = 2.6682868 + 3.7000365m$ and $\widehat{UCL}_3 = 0.908363 + 4.349375m$ where $\widehat{LWL}_3 = mn - \widehat{UWL}_3$ and $\widehat{LCL}_3 = mn - \widehat{UCL}_3$. The regression approach seems to provide good approximations that can be used in practice, at least as a starting point. For instance, for $m = 20$ and $n = 5$ we find $\widehat{UCL}_2 = 76.67$ for the RR_{2-of-2} scheme for the Shewhart MW chart. This value is close to the value 75 which was found using 10000 Monte Carlo simulations (see Table 1).

4.2 Performance of the charts

4.2.1 The in-control *ARL* robustness

One of the important appealing properties of a nonparametric control chart is its IC robustness property which means that the IC run-length distribution does not depend on the underlying process distribution. We study this property here in an extensive simulation study using a wide collection of continuous distributions, including non-normal distributions, light and heavy-tailed distributions, symmetric and asymmetric distributions, uni-modal, bi-modal distributions as well as some positively skewed distributions. Note that, wherever necessary, all distributions have been shifted and scaled such that the mean / median equals 0 and the standard

deviation equals 1, so that the results are easily comparable across the distributions. Specifically, the distributions considered in the study are:

- i. The standard normal distribution, $N(0,1)$.
- ii. The Student's t -distribution, $t(\nu)$, with degrees of freedom $\nu = 4$ and 8 , respectively, which is symmetric but with heavier tails than the Normal.
- iii. The gamma distribution, $GAM(\alpha, \beta)$, with parameters $(\alpha, \beta) = (1,1)$, is the exponential distribution, $EXP(1)$, which is positively skewed.
- iv. The Laplace (or double exponential) distribution, $DE(0,1)$ which is symmetric but with a different tail behavior than the normal.
- v. The log-normal distribution, $LogN(0,1)$, which is a heavy-tailed distribution.
- vi. The uniform distribution, $U(0,1)$, acknowledged as to be symmetric.

The attained ARL_0 values for the proposed charts, for these distributions, are shown in Table 2.

Table 2. Attained ARL_0 values for the RR_{1-of-1} , RR_{2-of-2} and IRR_{2-of-2} MW Shewhart charts with $LCL_1 = LCL_3 = 326$, $UCL_1 = UCL_3 = 2174$, $LCL_2 = LWL_3 = 650$, $UCL_2 = UWL_3 = 1850$ when $m = 500$ and $n = 5$

Distribution	ARL_0		
	RR_{1-of-1}	RR_{2-of-2}	IRR_{2-of-2}
$N(0,1)$	498.46	493.10	500.21
$DE(0,1)$	501.74	494.72	484.70
$U(0,1)$	495.56	499.27	498.37
$LogN(0,1)$	488.86	492.17	507.58
$GAM(1,1)$	500.12	498.27	496.97
$t(4)$	504.10	493.27	488.58
$t(8)$	498.83	497.28	492.46

From Table 2 it can be seen that, as expected, for every continuous distribution under consideration, the IC characteristics are almost equal; the difference between the values can be explained by simulation error. In practice we keep this error as small as possible (less than 10 percent of the nominal value of the ARL).

4.2.2 In-control and Out-of-control ARL

When using the ARL as the performance metric it is desirable to have a large attained ARL_0 and a small ARL_δ . The ARL can be calculated using Expression (9) by means of Monte Carlo simulations. However, since the run-length distribution is significantly right-skewed,

researchers have advocated using other more representative measures for the assessment of chart performance. These include the standard deviation of the run-length (*SDRL*) and other percentiles of the run-length, more specifically, the median run-length (*MRL*), which provides additional and more meaningful information about the in-control and out-of-control performances of control charts, not given by the *ARL*. The idea of looking at percentiles, in SPC, goes back to Barnard [17] and more recently researchers such as Gan [18], Chakraborti [19] and Khoo et al. [20] have advocated the use of percentiles, such as the median, for assessment of chart performance. Tables 3 and 4 give the *ARL*, *SDRL*, 5th, 25th, 50th, 75th and 95th percentiles of the run-length distribution for various distributions for Rule 1, the RR_{1-of-1} scheme, and Rule 2, the RR_{2-of-2} scheme, respectively. The results for Rule 3, the IRR_{2-of-2} scheme, are presented in Table 5. The first row of each cell gives the *ARL* and the *SDRL* values, respectively, whereas the second row gives the values of the 5th, 25th, 50th, 75th and 95th percentiles (in this order). The distribution with the best run-length characteristics is indicated using grey shading. When two or more columns are shaded it means that the charts perform similarly. This is done for all tables in this paper. Note that, for large shifts, the run-length characteristics converge toward one for the RR_{1-of-1} and IRR_{2-of-2} schemes and converge toward two for the RR_{2-of-2} scheme. The largest shift under consideration is $\delta = 2$, since the run-length characteristics converge for large shifts, with shifts of magnitude $\delta = 0.00(0.25)2.00$ being under consideration.

For all three rules the charts perform better under the *t*-distribution (with small degrees of freedom) than the standard normal distribution. As the degrees of freedom increases, the *t*- and standard normal distributions perform similarly, which is to be expected. For all three rules the charts perform best when the underlying process distribution is uniform. When considering the other distributions under consideration, there is a clear pattern in that the run-rules enhanced charts outperform the standard *I-of-I* chart for small to moderate shifts, which is to be expected.

Table 3. Characteristics of the run-length distribution for Rule 1, the RR_{1-of-1} scheme, for the Shewhart MW chart for $m = 500, n = 5, LCL_1 = 326$ and $UCL_1 = 2174$

Shift(δ)	$N(0,1)$	$LogN(0,1)$	$t(4)$	$t(8)$	$GAM(1,1)$	$U(0,1)$	$DE(0,1)$
0.00	498.46(531.34) 23,143,335,664,1522	488.86(502.61) 26,140,329,669,1486	504.10(525.99) 24,137,342,682,1530	498.83(523.81) 25,135,330,701,1482	500.12(529.36) 25,144,329,681,1588	495.56(548.49) 22,134,328,648,1613	501.74(523.19) 25,135,330,700,1548
0.25	197.86(216.20) 10,52,129,263,628	509.04(599.86) 23,125,316,656,1646	169.29(194.08) 7,45,109,225,526	185.74(201.38) 8,48,120,257,568	318.84(386.22) 14,78,192,408,1065	11.31(10.83) 1,4,8,15,34	287.70(324.38) 14,785,185,388,912
0.50	53.05(60.37) 3,14,34,69,169	230.53(284.58) 10,57,139,299,726	35.31(38.99) 2,9,23,47,114	47.26(52.16) 3,13,31,63,147	91.93(105.87) 4,23,57,122,287	1.82(1.22) 1, 1, 1, 2, 4	94.74(107.51) 5,24,60,128,30,309
0.75	16.22(16.25) 1, 5, 11, 22, 48	103.20(127.33) 5,25,61,132,341	9.50(9.44) 1,3,7,13,28	13.72(13.98) 1,4,9,19,42	26.68(30.32) 2,7,17,35,83	1.00(0.07) 1, 1, 1, 1, 1	31.56(35.14) 2,8,21,42,99
1.00	6.52(6.17) 1, 2, 5, 9, 19	42.33(51.06) 2,10,26,55,140	3.72(3.29) 1, 1, 3, 5, 10	5.50(5.15) 1, 2, 4, 7, 16	7.87(8.51) 1,2,5,10,24	1.00(0.00) 1, 1, 1, 1, 1	11.88(12.40) 1,4,8,16,36
1.50	2.05(1.44) 1, 1, 2, 3, 5	8.41(9.95) 1,2,5,11,27	1.47(0.84) 1, 1, 1, 2, 3	1.77(1.22) 1, 1, 1, 2, 4	1.39(0.84) 1, 1, 1, 2, 3	1.00(0.00) 1, 1, 1, 1, 1	3.19(2.81) 1, 1, 2, 4, 9
1.75	1.48(0.85) 1, 1, 1, 2, 3	4.15(4.63) 1, 1, 3, 5, 13	1.25(0.55) 1, 1, 1, 1, 2	1.37(0.72) 1, 1, 1, 2, 3	1.05(0.24) 1, 1, 1, 1, 1	1.00(0.00) 1, 1, 1, 1, 1	2.20(1.64) 1, 1, 2, 3, 5
2.00	1.19(0.47) 1, 1, 1, 1, 2	2.26(2.46) 1, 1, 1, 3, 6	1.13(0.39) 1, 1, 1, 1, 2	1.19(0.48) 1, 1, 1, 1, 2	1.00(0.07) 1, 1, 1, 1, 1	1.00(0.00) 1, 1, 1, 1, 1	1.71(1.12) 1, 1, 1, 2, 4

Table 4. Characteristics of the run-length distribution for Rule 2, the RR_{2-of-2} scheme, for the Shewhart MW chart for $m = 500, n = 5, LCL_2 = 650$ and $UCL_2 = 1850$

Shift(δ)	$N(0,1)$	$LogN(0,1)$	$t(4)$	$t(8)$	$GAM(1,1)$	$U(0,1)$	$DE(0,1)$
0.00	493.10(498.47) 25,140,323,660,1480	492.17(511.38) 27,145,334,666,1489	493.27(496.33) 22,137,345,653,1460	497.28(504.79) 24,143,342,681,1496	498.27(522.02) 24,132,332,679,1548	499.27(518.89) 29,141,338,687,1544	494.72(507.70) 24,127,338,687,1544
0.25	130.34(147.01) 7,35,84,177,404	214.69(262.18) 11,55,125,276,710	93.72(100.97) 6,25,62,123,302	121.85(139.34) 6,32,78,161,383	111.36(136.88) 7,29,70,144,350	7.73(6.52) 2, 3, 6, 10, 20	169.67(190.59) 8,44,108,228,558
0.50	28.06(28.83) 3,8,19,38,84	44.27(52.55) 3,12,28,56,140	15.73(14.60) 2,5,11,22,47	23.45(23.87) 2,7,16,31,71	16.37(17.35) 1,4,8,16,39	2.14(0.49) 2, 2, 2, 2, 3	39.80(42.41) 3,12,26,53,123
0.75	9.03(7.83) 2,4,7,12,25	11.21(11.76) 2, 4, 7,14,33	5.61(4.35) 2, 2, 4, 7, 14	7.61(6.69) 2, 3, 6, 10, 21	3.97(2.85) 2, 2, 3, 5, 10	2.00(0.00) 2, 2, 2, 2, 2	12.95(12.83) 2, 4, 9, 17, 38
1.00	4.41(3.19) 2, 2, 3, 6, 11	4.04(3.16) 2, 2, 3, 5, 10	3.27(1.90) 2, 2, 2, 4, 7	3.90(2.62) 2, 2, 3, 5, 9	2.23(0.70) 2, 2, 2, 2, 4	2.00(0.00) 2, 2, 2, 2, 2	6.46(5.41) 2, 3, 5, 8, 17
1.50	2.33(0.80) 2, 2, 2, 2, 4	2.04(0.31) 2, 2, 2, 2, 2	2.20(0.60) 2, 2, 2, 2, 4	2.28(0.78) 2, 2, 2, 2, 4	2.00(0.00) 2, 2, 2, 2, 2	2.00(0.00) 2, 2, 2, 2, 2	3.16(1.81) 2, 2, 2, 4, 7
1.75	2.11(0.44) 2, 2, 2, 2, 3	2.00(0.09) 2, 2, 2, 2, 2	2.08(0.37) 2, 2, 2, 2, 3	2.11(0.44) 2, 2, 2, 2, 3	2.00(0.00) 2, 2, 2, 2, 2	2.00(0.00) 2, 2, 2, 2, 2	2.55(1.08) 2, 2, 2, 3, 5
2.00	2.03(0.23) 2, 2, 2, 2, 2	2.00(0.00) 2, 2, 2, 2, 2	2.02(0.19) 2, 2, 2, 2, 2	2.04(0.25) 2, 2, 2, 2, 2	2.00(0.00) 2, 2, 2, 2, 2	2.00(0.00) 2, 2, 2, 2, 2	2.31(0.77) 2, 2, 2, 2, 4

Table 5. Characteristics of the run-length distribution for Rule 3, the IRR_{2-of-2} scheme, for the Shewhart MW chart for $m = 500, n = 5, LCL_3 = 650, LWL_3 = 326, UWL_3 = 1850$ and $UCL_3 = 2174$

Shift(δ)	$N(0,1)$	$LogN(0,1)$	$t(4)$	$t(8)$	$GAM(1,1)$	$U(0,1)$	$DE(0,1)$
0.00	500.21(544.02) 28,123,309,634,1508	507.58(534.33) 22,139,339,691,1515	488.58(502.52) 24,131,318,638,1487	492.46(505.52) 23,122,328,683,1532	496.97(500.39) 22,143,334,692,1520	498.37(500.81) 20,131,322,637,1567	484.70(498.25) 25,129,338,644,1409
0.25	130.13(142.18) 6,32,78,148,336	272.34(288.37) 23,143,326,654,1520	119.75(145.65) 5,31,78,167,403	130.51(131.97) 5,37,94,174,394	209.66(223.03) 11,54,135,267,584	11.86(12.27) 1,3,8,14,32	187.79(230.60) 14,785,185,388,912
0.50	33.51(38.48) 3,13,21,42,112	112.27(124.36) 7,39,102,223,528	24.84(24.19) 2,6,15,30,81	32.09(30.90) 2,10,23,43,96	57.79(67.24) 4,16,24,65,158	1.82(1.22) 1, 1, 1, 2, 4	63.14(70.23) 3,17,26,66,155
0.75	10.63(10.93) 1, 3, 8, 11, 30	65.05(80.44) 4,18,26,70,159	6.25(6.31) 1, 2, 5, 8,18	11.01(11.23) 1,3,8,15,30	16.33(18.52) 1,4,12,21,49	1.00(0.07) 1, 1, 1, 1, 1	25.13(28.49) 2,7,16,32,82
1.00	4.33(4.19) 1, 2, 3, 5, 10	28.89(35.09) 3,7,17,33,84	2.33(2.04) 1, 1, 2, 4, 6	4.29(3.57) 1, 2, 3, 6, 12	5.19(5.65) 1,2,4,6,15	1.00(0.00) 1, 1, 1, 1, 1	7.98(8.69) 1,2, 5, 11, 23
1.50	1.39(0.99) 1, 1, 2, 2, 3	11.23(12.35) 1, 3, 5, 15, 36	1.33(1.00) 1, 1, 1, 1, 2	1.66(1.09) 1, 1, 1, 2, 4	1.36(0.90) 1, 1, 1, 2, 3	1.00(0.00) 1, 1, 1, 1, 1	2.23(1.81) 1, 1, 2, 3, 9
1.75	1.33(0.78) 1, 1, 1, 1, 2	5.49(5.31) 1, 2, 4, 7, 16	1.25(0.51) 1, 1, 1, 1, 2	1.32(0.66) 1, 1, 1, 1, 3	1.04(0.21) 1, 1, 1, 1, 1	1.00(0.00) 1, 1, 1, 1, 1	1.72(1.22) 1, 1, 1, 2, 4
2.00	1.14(0.51) 1, 1, 1, 1, 2	3.11(2.50) 1, 1, 2, 4, 8	1.13(0.38) 1, 1, 1, 1, 2	1.13(0.39) 1, 1, 1, 1, 2	1.00(0.00) 1, 1, 1, 1, 1	1.00(0.00) 1, 1, 1, 1, 1	1.45(0.87) 1, 1, 1, 2, 3

Table 6. ARL values of the RR_{1-of-1} , RR_{2-of-2} and IRR_{2-of-2} Shewhart MW charts under the $N(0,1)$, $t(4)$ and $GAM(1,1)$ distributions for $m = 500$ and $n = 5$

Shifts	$N(0,1)$			$t(4)$			$GAM(1,1)$		
	RR_{1-of-1}	RR_{2-of-2}	IRR_{2-of-2}	RR_{1-of-1}	RR_{2-of-2}	IRR_{2-of-2}	RR_{1-of-1}	RR_{2-of-2}	IRR_{2-of-2}
0.00	498.46(531.34) 23,143,335,664,1522	493.10(498.47) 25,140,323,660,1480	500.21(544.02) 28,123,309,634,1508	504.10(525.99) 24,137,342,682,1530	493.27(496.33) 22,137,345,653,1460	488.58(502.52) 24,131,318,638,1487	500.12(529.36) 25,144,329,681,1588	498.27(522.02) 24,132,332,679,1548	496.97(500.39) 22,143,334,692,1520
0.25	197.86(216.20) 10,52,129,263,628	130.34(147.01) 7,35,84,177,404	130.13(142.18) 6,32,78,148,336	169.29(194.08) 7,45,109,225,526	93.72(100.97) 6,25,62,123,302	119.75(145.65) 5,31,78,167,403	318.84(386.22) 14,78,192,408,1065	111.36(136.88) 7,29,70,144,350	209.66(223.03) 11,54,135,267,584
0.50	53.05(60.37) 3,14,34,69,169	28.06(28.83) 3,8,19,38,84	33.51(38.48) 3,13,21,42,112	35.31(38.99) 2,9,23,47,114	15.73(14.60) 2,5,11,22,47	24.84(24.19) 2,6,15,30,81	91.93(105.87) 4,23,57,122,287	16.37(17.35) 1,4,8,16,39	57.79(67.24) 4,16,24,65,158
0.75	16.22(16.25) 1, 5, 11, 22, 48	9.03(7.83) 2,4,7,12,25	10.63(10.93) 1, 3, 8, 11, 30	9.50(9.44) 1,3,7,13,28	5.61(4.35) 2, 2, 4, 7, 14	6.25(6.31) 1, 2, 5, 8,18	26.68(30.32) 2,7,17,35,83	3.97(2.85) 2, 2, 3, 5, 10	16.33(18.52) 1,4,12,21,49
1.00	6.52(6.17) 1, 2, 5, 9, 19	4.41(3.19) 2, 2, 3, 6, 11	4.33(4.19) 1, 2, 3, 5, 10	3.72(3.29) 1, 1, 3, 5, 10	3.27(1.90) 2, 2, 2, 4, 7	2.33(2.04) 1, 1, 2, 4, 6	7.87(8.51) 1,2,5,10,24	2.23(0.70) 2, 2, 2, 4	5.19(5.65) 1,2,4,6,15
1.50	2.05(1.44) 1, 1, 2, 3, 5	2.33(0.80) 2, 2, 2, 4	1.39(0.99) 1, 1, 2, 3	1.47(0.84) 1, 1, 1, 2, 3	2.20(0.60) 2, 2, 2, 2, 4	1.33(1.00) 1, 1, 1, 1, 2	1.39(0.84) 1, 1, 1, 2, 3	2.00(0.00) 2, 2, 2, 2	1.36(0.90) 1, 1, 1, 2, 3
1.75	1.48(0.85) 1, 1, 1, 2, 3	2.11(0.44) 2, 2, 2, 3	1.33(0.78) 1, 1, 1, 1, 2	1.25(0.55) 1, 1, 1, 1, 2	2.08(0.37) 2, 2, 2, 2, 3	1.25(0.51) 1, 1, 1, 1, 2	1.05(0.24) 1, 1, 1, 1, 1	2.00(0.00) 2, 2, 2, 2	1.04(0.21) 1, 1, 1, 1, 1
2.00	1.19(0.47) 1, 1, 1, 1, 2	2.03(0.23) 2, 2, 2, 2	1.14(0.51) 1, 1, 1, 1, 2	1.13(0.39) 1, 1, 1, 1, 2	2.02(0.19) 2, 2, 2, 2, 2	1.13(0.38) 1, 1, 1, 1, 2	1.00(0.07) 1, 1, 1, 1, 1	2.00(0.00) 2, 2, 2, 2	1.00(0.00) 1, 1, 1, 1, 1

In Table 6 we compare the RR_{1-of-1} , RR_{2-of-2} and IRR_{2-of-2} Shewhart MW charts under the $N(0,1)$, $t(4)$ and $GAM(1,1)$ distributions. For small shifts, no matter the nature of the underlying distribution, the RR_{2-of-2} scheme performs best. For moderate shifts the IRR_{2-of-2} scheme performs best. For large shifts the RR_{1-of-1} and IRR_{2-of-2} schemes perform similarly and best, since the smallest value that their run-length can take on equals 1, whereas, for the RR_{2-of-2} scheme the smallest value that its run-length can take on equals 2, since at least two points are needed to give a signal. The results from Table 6 are illustrated in Figure 3 (d) – (f).

To illustrate the efficiency of the IRR_{2-of-2} and RR_{2-of-2} schemes we illustrate their performances under some of the distributions by presenting some graphs. Figures 1 (a), (b) and (c) show that the Shewhart MW chart is more efficient under non-normal distributions and we can see that the chart performs best under the uniform distribution.

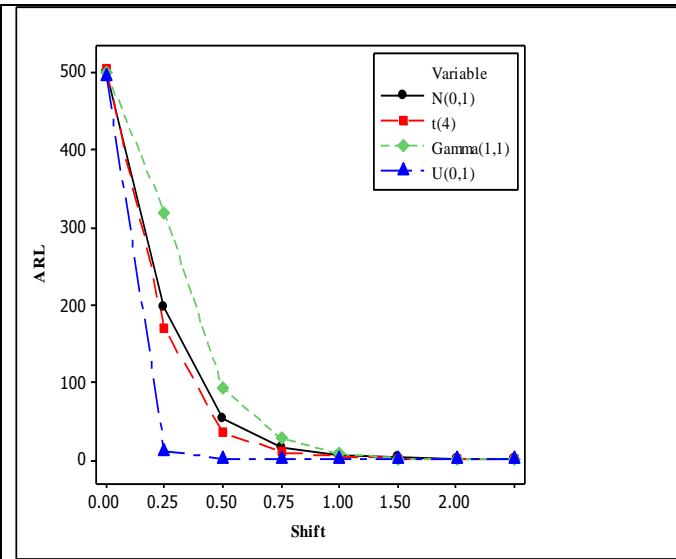


Figure 1 (a). ARL versus shift for the RR_{1-of-1} Shewhart MW control chart under the $N(0,1)$, $t(4)$, $GAM(1,1)$ and $U(0,1)$.

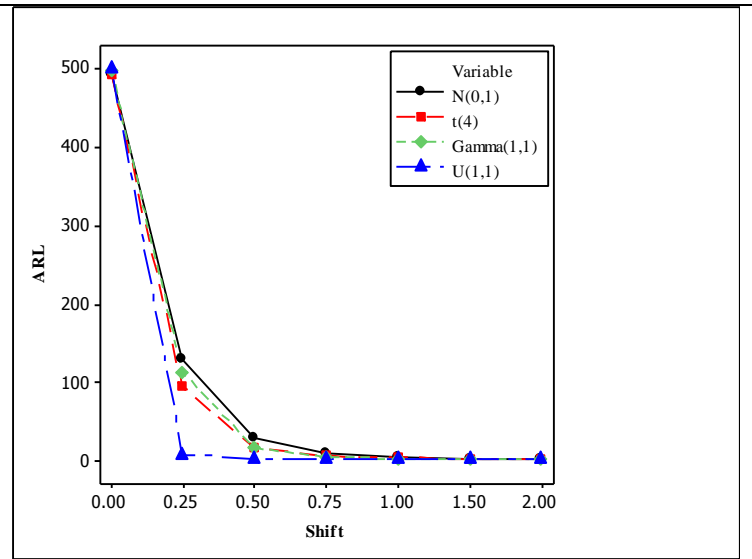


Figure 1(b). ARL versus shift for the RR_{2-of-2} Shewhart MW control chart under the $N(0,1)$, $t(4)$, $GAM(1,1)$ and $U(0,1)$.

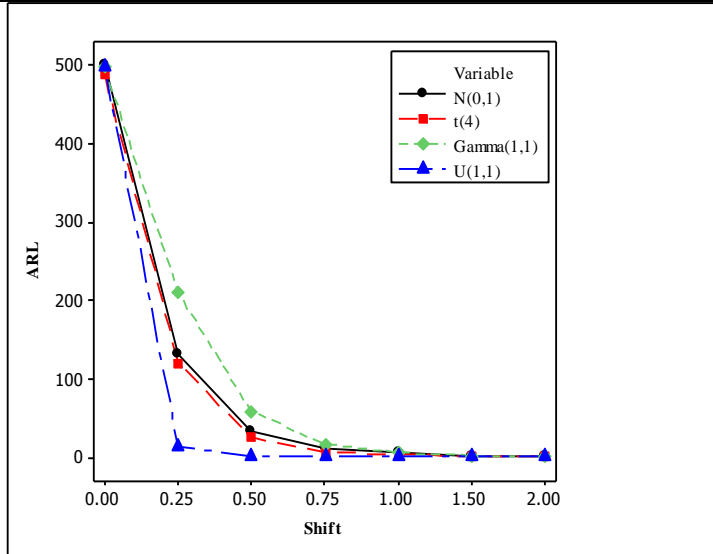


Figure 1 (c). ARL versus shift for the IRR_{2-of-2} Shewhart MW control chart under the $N(0,1)$, $t(4)$, $GAM(1,1)$ and $U(0,1)$.

5. Comparison of the MWRR control charts with other competing charts

It is meaningful to compare the runs-rule enhanced MW charts with other available nonparametric Shewhart-type charts. Thus we compare the RR_{1-of-1} , RR_{2-of-2} and IRR_{2-of-2} Shewhart MW charts to the RR_{1-of-1} and RR_{2-of-2} Shewhart precedence charts proposed by Chakraborti et al. [21] and Chakraborti et al. [10], respectively. In the latter papers the $N(0,1)$, $GAM(1,1)$ and $t(4)$ distributions were considered and, accordingly, the same distributions are considered here. For benchmarking, the parametric RR_{1-of-1} , RR_{2-of-2} and IRR_{2-of-2} Shewhart \bar{X} charts are also included in the performance comparison under the normal and non-normal distributions regardless of their non-robustness property (see Chakraborti et al. (2004)). The results are shown in Tables 7, 8 and 9, respectively.

From Table 7 it can be seen that, under the $N(0,1)$ distribution, the parametric Shewhart \bar{X} chart performs best. This is to be expected, since the underlying assumption of normality was met. Under the $t(4)$ and $GAM(1,1)$ distributions, see Tables 8 and 9, respectively, the RR_{2-of-2} Shewhart MW chart performs best for small to moderate shifts whereas the IRR_{1-of-1} Shewhart MW chart performs best for large shifts. The Shewhart precedence charts perform second best, whereas the parametric Shewhart \bar{X} chart performs worst. The results of Tables 7 to 9 are illustrated in Figures 2 (a) – (f) and 3 (a) – (c) where it can be seen that the parametric Shewhart \bar{X} charts perform best under normality and the Shewhart MW chart performs best when the underlying process distribution is non-normal.

Table 7. *ARL* and *SDRL* values for the RR_{1-of-1} and RR_{2-of-2} Shewhart \bar{X} , MW and precedence charts for the $N(0,1)$ distribution when $m = 500$, $j = 3$ and $n = 5$

Shift (δ)	Rule 1: RR_{1-of-1}						Rule 2: RR_{2-of-2}						Rule 3: IRR_{2-of-2}					
	Shewhart \bar{X}		MW		Precedence		Shewhart \bar{X}		MW		Precedence		Shewhart \bar{X}		MW		Precedence	
	<i>ARL</i>	<i>SDRL</i>	<i>ARL</i>	<i>SDRL</i>	<i>ARL</i>	<i>SDRL</i>	<i>ARL</i>	<i>SDRL</i>	<i>ARL</i>	<i>SDRL</i>	<i>ARL</i>	<i>SDRL</i>	<i>ARL</i>	<i>SDRL</i>	<i>ARL</i>	<i>SDRL</i>	<i>ARL</i>	<i>SDRL</i>
0.00	500.00	511.14	498.46	531.34	520.27	613.67	502.37	519.24	493.10	498.47	490.21	554.18	523.19	599.63	500.21	544.02	505.24	722.71
0.25	184.12	216.66	197.86	216.20	261.60	329.17	117.00	122.92	130.34	147.01	170.07	203.00	179.98	198.68	130.13	142.18	142.50	149.69
0.50	43.38	48.51	53.05	60.37	77.73	95.38	23.48	21.96	28.06	28.83	39.37	43.17	33.04	40.61	33.51	38.48	33.14	27.94
0.75	13.12	13.71	16.22	16.25	25.79	29.64	7.68	6.78	9.03	7.83	12.99	12.60	18.17	19.06	10.63	10.93	18.23	19.48
1.00	5.19	4.93	6.52	6.17	10.26	10.93	3.89	2.66	4.41	3.19	5.99	4.90	4.12	4.83	4.33	4.19	6.04	5.03
1.50	1.67	1.08	2.05	1.44	2.76	2.34	2.22	0.62	2.33	0.80	2.67	1.26	1.36	1.03	1.39	0.99	2.12	1.59
2.00	1.09	0.32	1.19	0.47	1.39	0.75	2.01	0.16	2.03	0.23	2.10	0.41	1.09	0.31	1.14	0.51	1.48	0.95

Table 8. *ARL* and *SDRL* values for the RR_{1-of-1} and RR_{2-of-2} Shewhart \bar{X} , MW and precedence charts for the $t(4)$ distribution when $m = 500$, $j = 3$ and $n = 5$

Shift (δ)	Rule 1: RR_{1-of-1}						Rule 2: RR_{2-of-2}						Rule 3: IRR_{2-of-2}					
	Shewhart \bar{X}		MW		Precedence		Shewhart \bar{X}		MW		Precedence		Shewhart \bar{X}		MW		Precedence	
	<i>ARL</i>	<i>SDRL</i>	<i>ARL</i>	<i>SDRL</i>	<i>ARL</i>	<i>SDRL</i>	<i>ARL</i>	<i>SDRL</i>	<i>ARL</i>	<i>SDRL</i>	<i>ARL</i>	<i>SDRL</i>	<i>ARL</i>	<i>SDRL</i>	<i>ARL</i>	<i>SDRL</i>	<i>ARL</i>	<i>SDRL</i>
0.00	517.60	27217.13	504.10	525.99	520.27	613.67	538.55	798.03	493.27	496.33	490.21	554.18	535.06	992.25	488.58	502.52	497.48	644.07
0.25	361.12	81.30.44	169.29	194.08	328.18	426.13	181.58	508.52	93.72	100.97	138.19	170.25	348.48	883.42	119.75	145.65	153.56	195.67
0.50	397.43	60026.60	35.31	38.99	117.63	167.75	445.18	886.59	15.73	14.60	25.09	27.66	220.68	800.24	24.84	24.19	46.88	54.93
0.75	161.54	20545.26	9.50	9.44	37.43	53.44	115.42	297.59	5.61	4.35	7.43	6.66	74.25	341.64	6.25	6.31	15.93	18.28
1.00	93.91	14137.58	3.72	3.29	12.58	16.84	41.83	12.74	3.27	1.90	3.61	2.36	36.54	300.28	2.33	2.04	6.32	6.61
1.50	41.93	6250.00	1.47	0.84	2.40	2.20	18.57	896.44	2.20	0.60	2.17	0.55	8.79	108.94	1.33	1.00	1.84	1.42
2.00	36.1	5672.63	1.13	0.39	1.18	0.49	2.06	1.93	2.02	0.19	2.02	0.16	4.23	86.61	1.13	0.38	1.11	0.39

Table 9. *ARL* and *SDRL* values for the RR_{1-of-1} and RR_{2-of-2} Shewhart \bar{X} , MW and precedence charts for the $GAM(1,1)$ distribution when $m = 500$, $j = 3$ and $n = 5$

Shift (δ)	Rule 1: RR_{1-of-1}						Rule 2: RR_{2-of-2}						Rule 3: IRR_{2-of-2}					
	Shewhart \bar{X}		MW		Precedence		Shewhart \bar{X}		MW		Precedence		Shewhart \bar{X}		MW		Precedence	
	<i>ARL</i>	<i>SDRL</i>	<i>ARL</i>	<i>SDRL</i>	<i>ARL</i>	<i>SDRL</i>	<i>ARL</i>	<i>SDRL</i>	<i>ARL</i>	<i>SDRL</i>	<i>ARL</i>	<i>SDRL</i>	<i>ARL</i>	<i>SDRL</i>	<i>ARL</i>	<i>SDRL</i>	<i>ARL</i>	<i>SDRL</i>
0.00	509.21	608.57	500.12	529.36	520.27	613.67	456.89	577.77	498.27	522.02	490.21	554.18	480.75	555.25	496.97	500.39	502.33	718.10
0.25	204.85	241.37	318.84	386.22	600.16	844.59	123.27	141.52	111.36	136.88	310.12	405.49	225.70	242.90	209.66	223.03	236.98	313.90
0.50	85.99	100.81	91.93	105.87	290.46	406.50	29.55	30.47	16.37	17.35	88.52	111.41	91.28	109.67	57.79	67.24	121.54	154.47
0.75	37.03	42.78	26.68	30.32	141.80	196.68	9.94	9.24	3.97	2.85	28.03	33.05	55.07	69.65	16.33	18.52	58.53	70.34
1.00	16.79	18.82	7.87	8.51	69.72	95.80	4.55	3.51	2.23	0.70	10.26	10.74	39.04	47.37	5.19	5.65	30.20	36.38
1.50	4.19	4.11	1.39	0.84	17.67	23.33	2.09	0.39	2.00	0.00	2.61	1.34	6.96	6.93	1.36	0.90	7.05	8.76
2.00	1.53	0.98	1.00	0.07	4.96	5.92	2.00	0.00	2.00	0.00	2.00	0.03	2.53	1.82	1.00	0.00	2.55	2.65

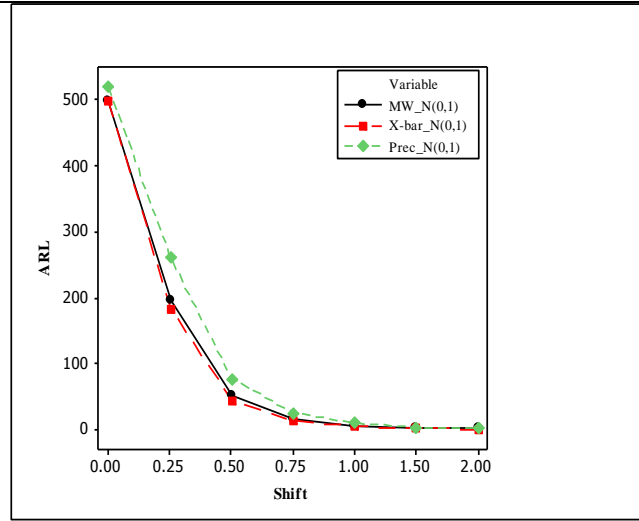


Figure 2(a). *ARL* versus shift for the RR_{1-of-1} Shewhart \bar{X} , precedence and MW charts under the standard normal distribution for $m = 500$ and $n = 5$.

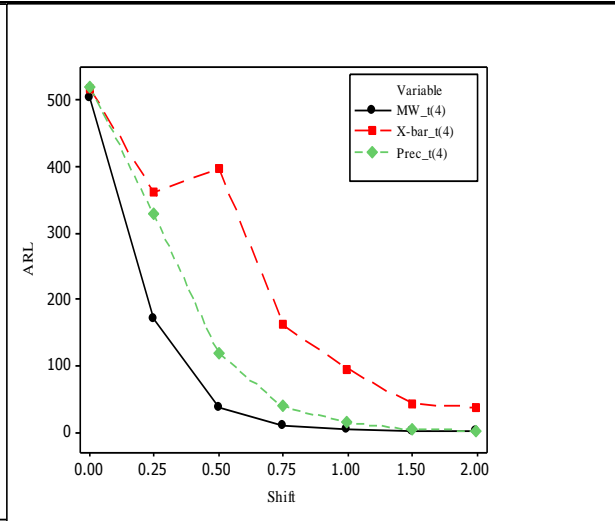


Figure 2(c). *ARL* versus shift for the RR_{1-of-1} Shewhart \bar{X} , precedence and MW charts under the $t(4)$ distribution for $m = 500$ and $n = 5$.

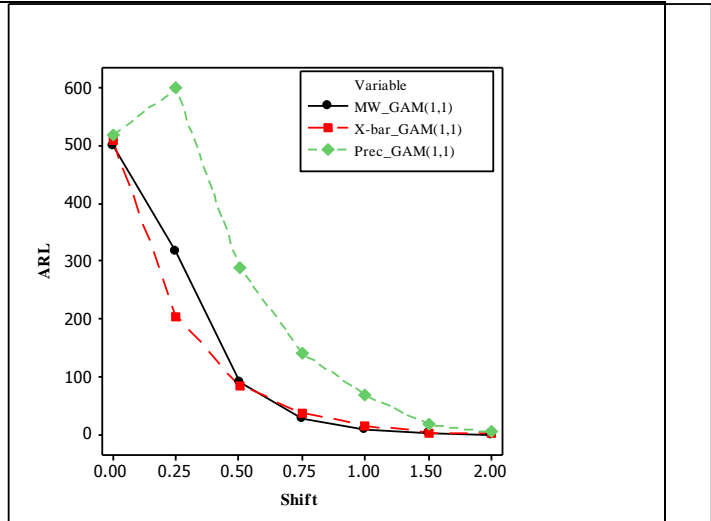


Figure 2(e). *ARL* versus shift for the RR_{1-of-1} Shewhart \bar{X} , precedence and MW charts under the $GAM(1,1)$ distribution for $m = 500$ and $n = 5$.

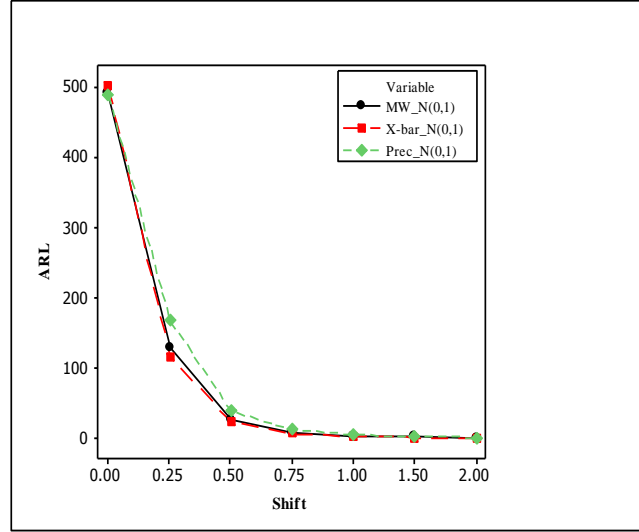


Figure 2(b). *ARL* versus shift for the RR_{2-of-2} Shewhart \bar{X} , precedence and MW charts under the standard normal distribution for $m = 500$ and $n = 5$.

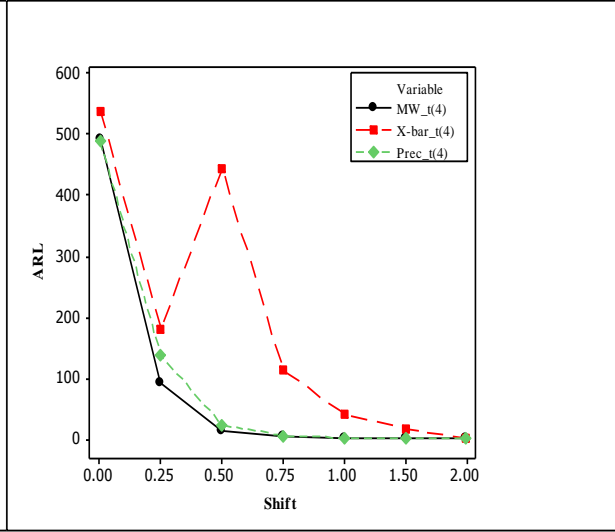


Figure 2(d). *ARL* versus shift for the RR_{2-of-2} Shewhart \bar{X} , precedence and MW charts under the $t(4)$ distribution for $m = 500$ and $n = 5$.

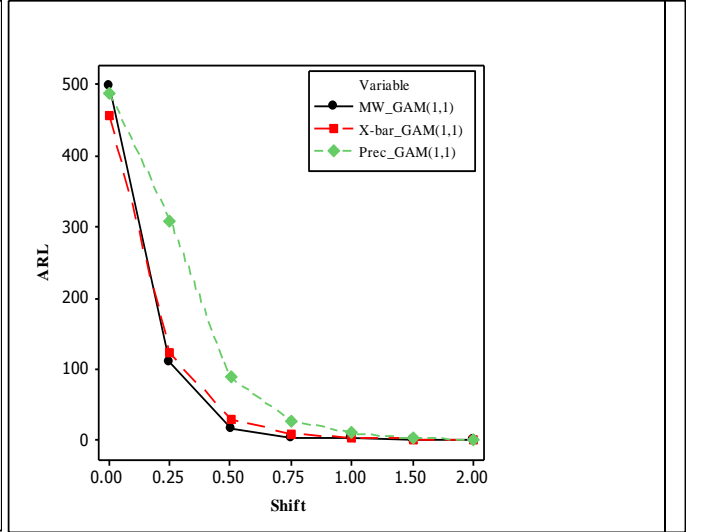


Figure 2(f). *ARL* versus shift for the RR_{2-of-2} Shewhart \bar{X} , precedence and MW charts under the $GAM(1,1)$ distribution for $m = 500$ and $n = 5$.

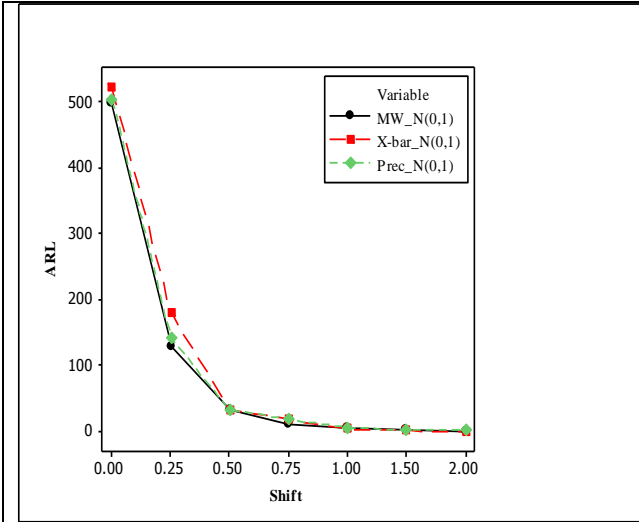


Figure 3(a). ARL versus shift for the IRR_{2-of-2} Shewhart \bar{X} , precedence and MW charts under the $GAM(1,1)$ distribution for $m = 500$ and $n = 5$.

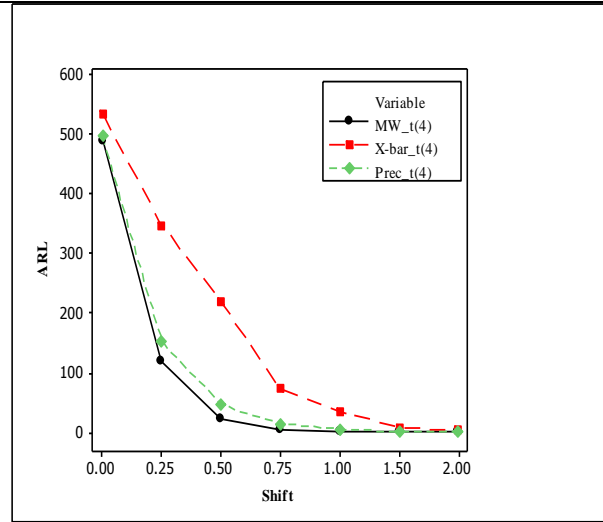


Figure 3(b). ARL versus shift for the IRR_{2-of-2} Shewhart \bar{X} , precedence and MW charts under the $t(4)$ distribution for $m = 500$ and $n = 5$.

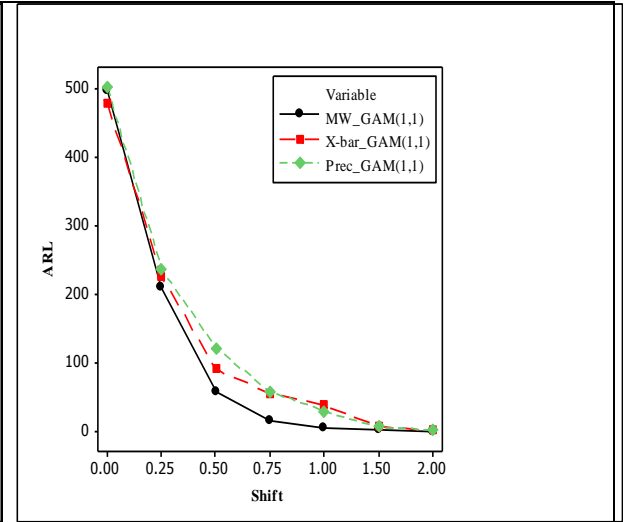


Figure 3(c). ARL versus shift for the IRR_{2-of-2} Shewhart \bar{X} , precedence and MW charts under the $t(4)$ distribution for $m = 500$ and $n = 5$.

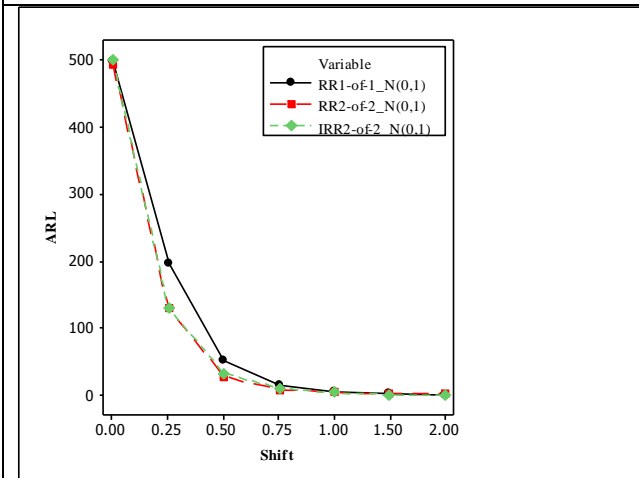


Figure 3(d). Performance comparison of the RR_{1-of-1} , RR_{2-of-2} and IRR_{2-of-2} MW charts under the standard normal distribution for $m = 500$ and $n = 5$.

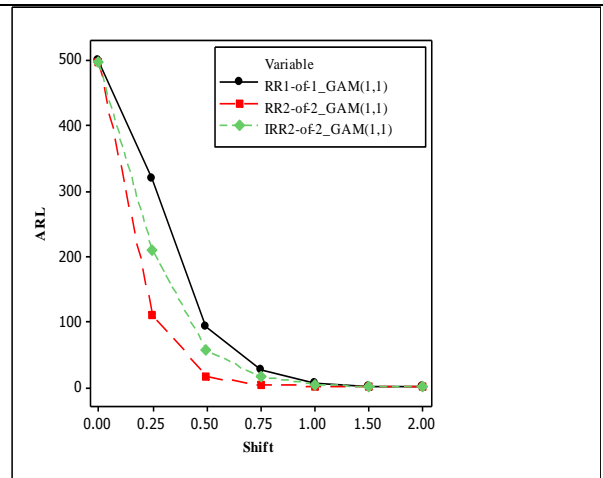


Figure 3(e). Performance comparison of the RR_{1-of-1} , RR_{2-of-2} and IRR_{2-of-2} MW charts under the $GAM(1,1)$ distribution for $m = 500$ and $n = 5$.

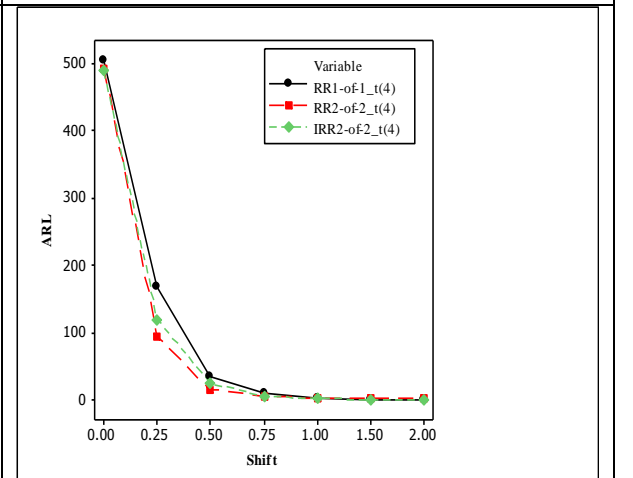


Figure 3(f). Performance comparison of the RR_{1-of-1} , RR_{2-of-2} and IRR_{2-of-2} MW charts under the $t(4)$ distribution for $m = 500$ and $n = 5$.

6. Illustrative example

We illustrate the implementation of the proposed distribution-free charts using a well-known dataset from Montgomery [22; page 223; Tables 5.2 and 5.3]. The data are the inside diameters of piston rings manufactured by a forging process. The data given in Table 5.2 contains fifteen prospective (Phase II) samples, each of size $n = 5$. Table 5.3 contains 125 retrospective or Phase I observations, that were collected when the process was considered IC ($m = 125$). These data are considered to be the Phase I reference data for which a goodness of fit test for normality is not rejected.

For the RR_{1-of-1} Shewhart MW chart, for an $ARL_0 \approx 500$, the lower and upper control limits are given by 80 and 545, respectively, which yield an ARL_0 of 492.68. A plot of the MW charting statistics is shown in Figure 4. It is seen that the RR_{1-of-1} Shewhart MW chart signals for the first time on the 12th sample in the prospective phase.

For the RR_{2-of-2} Shewhart MW chart, for a nominal ARL_0 of 500, we find $LCL_2 = 160$ and $UCL_2 = 465$ which yields an ARL_0 of 499.92. A plot of the MW charting statistics is shown in Figure 4. It is seen that the RR_{2-of-2} Shewhart MW chart signals for the first time on the 9th sample in the prospective phase. Thus, the RR_{2-of-2} scheme performs better than the RR_{1-of-1} scheme.

Using the same dataset Malela-Majika et al. [16] showed that the Min chart signals on the 13th sample in the retrospective phase, whereas the precedence chart based on the median signals on the 9th sample in the prospective phase. This confirms again that the RR_{2-of-2} Shewhart MW chart performs better than its competitors for these data.

For the IRR_{2-of-2} Shewhart MW chart, for a nominal ARL_0 of 500, we find $LCL_3 = 80$, $LWL_3 = 160$, $UWL_3 = 465$ and $UCL_3 = 545$ which yields an ARL_0 of 497.81. A plot of the MW charting statistics is shown in Figure 4. It is seen that the IRR_{2-of-2} Shewhart MW chart signals for the first time on the 9th sample in the prospective phase. Thus, the IRR_{2-of-2} and the RR_{2-of-2} schemes perform better than the RR_{1-of-1} scheme.

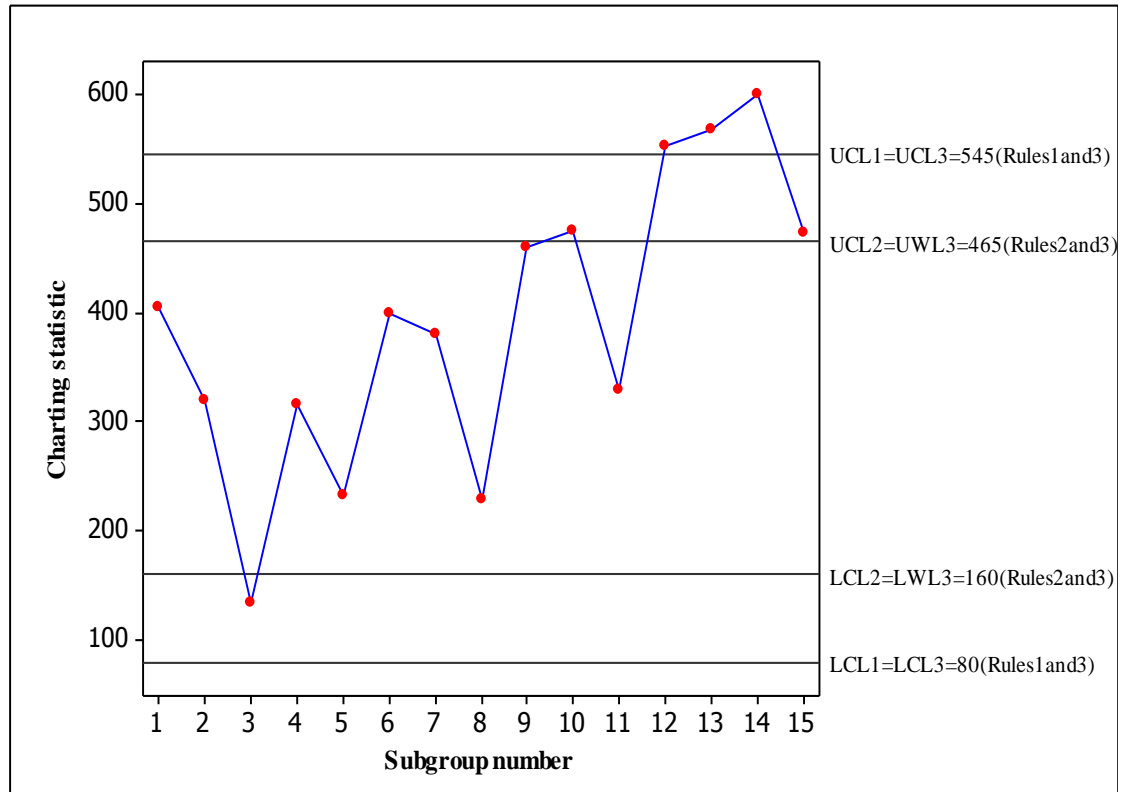


Figure 4. The RR_{1-of-1} , RR_{2-of-2} and IRR_{2-of-2} Shewhart MW charts for the Montgomery (2005) piston ring data

7. Conclusion and remarks

In this paper, we consider enhancing the performance of the Phase II Shewhart-type distribution-free chart based on the well-known Mann-Whitney statistic the Shewhart MW chart, considered by Chakraborti and Van de Wiel [1], by adding standard and improved runs-rules. A performance comparison of the runs-rules enhanced Shewhart MW charts with the existing parametric and nonparametric Shewhart-type charts shows that the enhanced charts perform better in detecting shifts under distributions of various shapes. Thus, on the basis of practicality, minimal assumptions, robustness of the in-control run-length distribution and out-of-control performance, the runs-rules enhanced Shewhart MW charts are strong contenders in practical SPC applications. Note that, the focus in this article has been on the standard and improved runs-rules and enhancements of the Phase II Shewhart-type distribution-free charts. Adaptations to the scenario, such as the modified runs-rules proposed by Antzoulakos and Rakitzis [23] are currently being investigated and will be reported in a separate paper.

Acknowledgements

This work formed a part of the first author's Master's dissertation at the University of Pretoria and was supported by a bursary from the South African Research Chair Initiative (SARChI) funds awarded to the second author at the Department of Statistics at the University of Pretoria. The research of the third author was partly supported by a National Research Foundation grant (Reference: TTK14061168807, UID: 94102).

References

- [1] Chakraborti S, Van de Wiel MA (2008) A nonparametric control chart based on the Mann-Whitney statistic. *IMS Collections. Beyond Parametrics in Interdisciplinary Research: Festschrift in Honor of Professor Pranab K. Sen* 1:156-172.
- [2] Gibbons JD, Chakraborti S (2010) *Nonparametric Statistical Inference*, 5th ed., Taylor and Francis, Boca Rator, FL.
- [3] Park C Reynolds Jr MR (1987) Nonparametric procedures for monitoring a location parameter based on linear placement statistics. *Sequential Analysis* 6(4):303-323.
- [4] Zhou C, Zou C, Zhang Y, Wang Z (2009) Nonparametric control chart based on change-point model. *Stat Pap* 50(1):13-28.
- [5] Li SY, Tang LC, Ng SH (2010) 'Nonparametric CUSUM and EWMA control charts for detecting mean shifts'. *J Qual Technol* 42(2):209-226.
- [6] Champ CW, Woodall WH (1987) Exact results for Shewhart control charts with supplementary runs rules. *Technometrics* 29(4):393-399.
- [7] Klein M (2000) Two alternatives to Shewhart \bar{X} control chart. *J Qual Technol* 32: 27-431.
- [8] Khoo MBC, Ariffin KN (2006) Two improved runs rules for Shewhart \bar{X} control chart. *Quality Engineering* 18:173-178.
- [9] Koutras MV, Bersimis S, Maravelakis PE (2007) Statistical process control using Shewhart control charts with supplementary runs rules. *Methodology and Computing in Applied Probability* 9:207-224.
- [10] Chakraborti S, Eryilmaz S, Human SW (2009) A phase II nonparametric control chart based on precedence statistics with runs-type signaling rules. *Comput Stat Data An* 53(4):1054-1065.
- [11] Zhang Y, Castagliola P (2010) Run rules \bar{X} charts when process parameters are unknown. *International Journal of Reliability, Quality and Safety Engineering* 17(4):381–399.

- [12] Chakraborti S, Van der Laan P, Bakir ST (2001) Nonparametric control charts: An overview and some results. *J Qual Technol* 33(3):304-315.
- [13] Chakraborti S, Graham MA (2007) Nonparametric control charts. *Encyclopedia of Statistics in Quality and Reliability* 1:415 – 429, John Wiley, New York.
- [14] Chakraborti S, Human SW, Graham MA (2011) Nonparametric (distribution-free) quality control charts. In *Handbook of Methods and Applications of Statistics: Engineering, Quality Control, and Physical Sciences*. N. Balakrishnan, Ed., 298-329, John Wiley & Sons, New York.
- [15] Derman C, Ross SM (1997) *Statistical Aspects of Quality Control*, San Diego: Academic Press.
- [16] Malela-Majika JC, Chakraborti S, Graham MA (2015) Distribution-free precedence control charts with improved runs-rules. Submitted.
- [17] Barnard GA (1959) Control charts and stochastic processes. *J Roy Stat Soc B* 21(2):239-271.
- [18] Gan FF (1994) An optimal design of cumulative sum control chart based on median run length. *Commun Stat Simulat* 23(2):485 - 503.
- [19] Chakraborti S (2007) Run length distribution and percentiles: The Shewhart \bar{X} chart with unknown parameters. *Quality Engineering* 19(2):119-127.
- [20] Khoo MBC, Wong VH, Wu Z, Castagliola P (2011) Optimal designs of the multivariate synthetic chart for monitoring the process mean vector based on median run length. *Qual Reliab Eng Int* 27(8):981-997.
- [21] Chakraborti S, Van der Laan P, Van de Wiel MA (2004) A class of distribution-free control charts. *J Roy Stat Soc C-App*, 53(3):443-462.
- [22] Montgomery DC (2005) *Introduction to Statistical Quality Control*, 5th Edition, John Wiley, New York, NY.
- [23] Antzoulakos DL, Rakitzis AC (2008) The modified r out of m control chart. *Commun Stat Simulat* 37(2):396-408.